Journal of Hazardous Materials 183 (2010) 224–232

Contents lists available at ScienceDirect

Journal of Hazardous Materials

journal homepage: www.elsevier.com/locate/jhazmat

Behaviors and mechanism of acid dyes sorption onto diethylenetriamine-modified native and enzymatic hydrolysis starch

Zuohua Wang, Bo Xiang*, Rumei Cheng, Yijiu Li

Department of Chemistry, Tongji University, Shanghai 200092, China

ARTICLE INFO

Article history:
Received 19 May 2010
Received in revised form 1 July 2010
Accepted 2 July 2010
Available online 1 August 2010

Keywords:
Diethylenetriamine
Enzymatic hydrolysis
Modified starch
Acid dyes
Sorption mechanism

ABSTRACT

In this paper, different starches were modified by diethylenetriamine. The native starch reacted with diethylenetriamine giving CAS, whereas the enzymatic hydrolysis starch was modified by diethylenetriamine producing CAES. Adsorption capacities of CAES for four acid dyes, namely, Acid orange 7 (AO7), Acid orange 10 (AO10), Acid green 25 (AG25) and Acid red 18 (AR18) have been determined to be 2.521, 1.242, 1.798 and 1.570 mmol g^{-1}, respectively. In all cases, CAES has exhibited higher sorption ability than CAS, and the increment for these dyes took the sequence of AO7 (0.944 mmol g^{-1}) > AO10 (0.592 mmol g^{-1}) > AR18 (0.411 mmol g^{-1}) > AG25 (0.047 mmol g^{-1}). Sorption kinetics and isotherms analysis showed that these sorption processes were better fitted to pseudo-second-order equation and Langmuir equation. Chemical sorption mechanisms were confirmed by studying the effects of pH, ionic strength and hydrogen bonding. Thermodynamic parameters of these dyes onto CAES and CAS were also observed and it indicated that these sorption processes were exothermic and spontaneous in nature.

1. Introduction

Each year over 7×10^5 ton of dyestuffs is produced, and it is estimated that around 10–15% of the dyes are lost in the effluent during the dyeing processes [1,2] to cause serious environmental problems. Besides that, many of the dyestuffs have been reported to be toxic, carcinogenic or mutagenic to human beings [3,4]. Acid dyes are widely used in various fields due to their excellent stability during washing and their simple dyeing procedures. Most of them have a complex aromatic molecular structure such as benzene, naphthalene, anthracene, toluene, xylene, and so on. These stable aromatic structures of the dyes make them difficult to be biodegraded [5,6].

So far, various techniques such as coagulation [7], oxidation [8], photo degradation [9], and adsorption [10] have been applied to treat dye-containing effluents. Among these methods, adsorption technique has been recognized as an effective, efficient and economic method for its simple operation and better results [10–12]. A number of non-conventional, low-cost adsorbents have been tried for removal of dyes from wastewater, including agricultural solid wastes [13,14], clays [15], siliceous materials [16,17] and zeolites [18]. Recently, natural polymers are gaining interest for application as adsorbents due to their biodegradable and non-toxic nature [19]. As an abundant, inexpensive and renewable natural raw material, starch has attracted much attention for dye removal [20–22]. Cationic starches are found to be effective adsorbents for anionic dye waters. It was found that cationic starch with a higher DS had higher adsorption capacity [23]. Some researches have also mentioned that the presence of amino groups on the starch and the structure of the dyes could influence the adsorption capacity [24] without further detailed investigation. In order to get the adsorption mechanism and relationship between dye structure and adsorption capacity, our research group has done some relative research.

In the previous work of our group, a series of polyamine-modified starches containing amine groups has been synthesized. We have also proved that those starch derivants containing amine groups could effectively remove heavy metals and dyes from aqueous solutions [25,26]. In this study, native starch and enzymatic hydrolysis starch were reacted with diethylenetriamine to produce cross-linked amined starch (CAS) and cross-linked amined enzyme-hydrolyzed starch (CAES), respectively. To the best of our knowledge, there have been few literatures about the adsorption of CAES for dyes removal, and the sorption mechanism of CAES toward acid dyes has not been reported up to now. Therefore, the aim of this study is to investigate the behaviors of dyes onto CAES by studying their adsorption procedures and obtain new insights into the intermolecular interaction between dyes and amino-starches by a sorption comparison. Four acid dyes in common usage were employed in this work: AO7, AO10, AG25 and AR18, which were

* Corresponding author. Tel.: +86 021 65983695; fax: +86 021 65983695.
E-mail address: bxiangbo@tongji.edu.cn (B. Xiang).

0304-3894/$ – see front matter © 2010 Elsevier B.V. All rights reserved.
doi:10.1016/j.jhazmat.2010.07.015

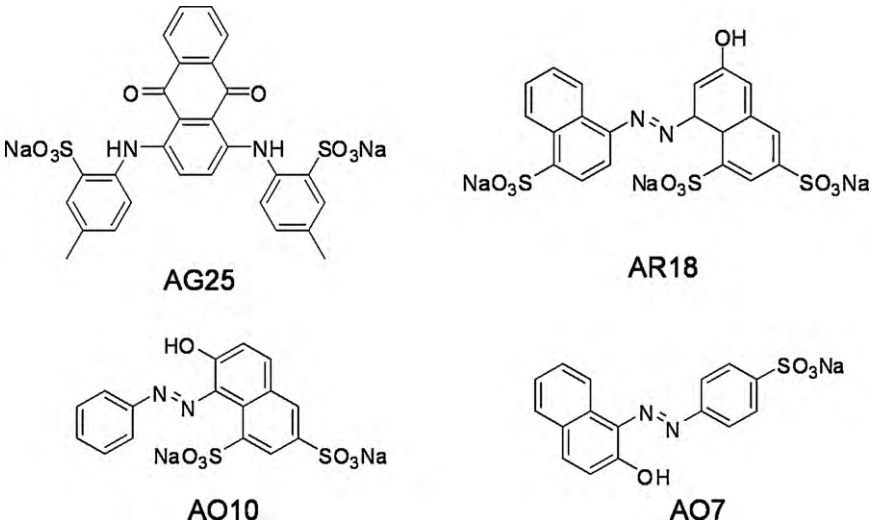

Fig. 1. Chemical structure of acid dyes used in this study.

regarded as typical reactive dye contaminants in the discharged effluent, and accordingly were widely studied [27,28].

2. Experimental

2.1. Materials

Commercial corn starch, of food-grade quality, was used in this study. Four commercially available textile dyestuffs were used in this research including three azo dyes (AO10, AO7 and AR18) and one anthraquinone dye (AG25). The chemical structures of them are shown in Fig. 1. All dyestuffs were obtained from Sigma and used without further purification. Characteristics of adsorbates and adsorbents are listed in Table 1.

2.2. Techniques

UV–vis spectra were measured on Agilent-8453 Spectrometer. Fourier transform infrared spectra were recorded on Nicolet FTIR NEXUS spectrometer with KBr pellets in the 4000–500 cm^{-1} regions. X-ray diffraction (XRD) measurements were carried out on a Rigaku D/max 2550 V instrument with Cu Kα radiation (λ = 1.5406 Å). Elemental content was determined with a PerkinElmer organic element analyzer. Specific surface area was determined by TRISTAR3000 BET determinator and obtained by equation of BET (Brunauer–Emmett–Teller).

2.3. Preparation of the enzymatic hydrolysis starch (ES)

30 g corn starch was immersed in the buffer solution (sodium citrate–disodium hydrogen phosphate, pH ≈ 5.0) with stirring to form a starch suspension. Next, 1 g admixture of glucoamylase and α-amylase (5:1, w/w) was added to the suspension. Following that, the mixture was kept stirring for 4 h at 45 °C in a water bath. After that, 5 mL sodium hydroxide solution (4%) was dropped to stop the enzymolysis. Then the enzymatic hydrolysis starch was filtrated from the mixture and washed several times with distilled water, and dried at 45 °C under vacuum for 24 h to give the enzymatic hydrolysis starch powder (ES).

2.4. Preparation of the adsorbents

The synthesis of CAS and CAES was according to literature [29]. The cross-linked starch (CS) or cross-linked enzymatic hydrolysis starch (CES) was synthesized by reacting 100 g corn starch/ES with 8.0 mL epichlorohydrin (ECH) in 200 mL dilute caustic solution for 18 h under 25 °C, then the pH was adjusted to neutral, and the CS/CES was separated from solution. The intermediate, 3-chloro-2-hydroxypropyl cross-linked starch (CHCS) or 3-chloro-2-hydroxypropyl cross-linked enzymatic hydrolysis starch (CHCES) was prepared from dried CS/CES with ECH in the presence of $HClO_4$ (the molar ratio was CS/CES:ECH:$HClO_4$ = 1:3:0.04) at 90 °C for 16 h. The dried CHS/CHCES was further reacted with diethylenetriamine to produce diethylenetriamine-modified starch (CAS) or diethylenetriamine-modified enzymatic hydrolysis starch (CAES) in basic solution under 60 °C for 4 h. This product was adjusted to neutral using HCl (1%), NaOH (1%), and was washed with deionized water, acetone successively. Then the acquired CAS/CAES was dried at 60 °C under vacuum for 24 h.

2.5. Adsorption procedure

All batch experiments were performed in the thermostatic shaker bath with a shaking of 200 rpm. Apart from the investigation for the effect of temperature on the sorption, all the other batch experiments were agitated for 12 h at 25 °C. For kinetic studies, 800 mg L^{-1} dye solutions (200 mL, pH 4.0) were agitated with 0.15 g of adsorbents for predetermined intervals of time, respec-

Table 1
Characteristics of the adsorbates and adsorbents used in this study.

Adsorbates			Adsorbents		
Generic name	Abbreviation	Fw		Content of $-NH_2$ (mmol g^{-1})	BET surface area (m^2 g^{-1})
Acid orange 7	AO7	350.3	CAS	2.24	0.4346
Acid orange 10	AO10	452.4			
Acid green 25	AG25	622.6	CAES	3.86	0.5012
Acid red 18	AR18	604.5			

tively. For equilibrium adsorption studies, a fix mass of adsorbent (20 mg) was weighted into flasks and contacted with a known concentration (300–1500 mg L^{-1}) of 25 mL dye solutions at pH 4. The influence of pH on acid dyes removal was observed by adjusting dye solutions (500 mg L^{-1}) to a pH range of 3–12 and agitating 25 mL of dye solutions with 0.015 g of adsorbent. For the effect of ionic strength, experiments were carried out by agitating 100 mL of various dye solutions with known amounts of sodium sulfate (10^{-5} to 10^{-1} mol L^{-1}) and fix dye initial concentration of 10^{-4} mol L^{-1}. Effect of hydrogen bonding was observed by studying the spectra shift of each dye solutions (10^{-4} mol L^{-1}) in different solvents (methanol, water and dimethylsulfoxide) and on CAES. The diffuse reflectance signal of the dyes on CAES was converted to the absorbance scale using software provided with the instrument. The effect of temperature over a range of 20–45 °C on dye removal was carried out in 25 mL of dye solutions (500 mg L^{-1}, pH 4.0) with 0.025 g of adsorbent. After filtration, the concentration of each dye solution was determined. The amount of adsorbed dyes was calculated using the following Eq. (1):

$$q_e = \frac{(C_0 - C_1) \times V}{m} \quad (1)$$

where q_e is the amount of absorbed dyes (mg/g); C_0 and C_1 are the initial and residual concentration (mg L^{-1}), respectively; V is the volume of dyes aqueous solution (L); m is the dose of adsorbent (g).

3. Results and discussion

3.1. Characteristic of the products

The preparation of CAES was gained by enzymolysis and diethylenetriamine modification of native starch. Products in each step were analyzed by FTIR and XRD. The FTIR spectra (Fig. 2) of CES and CHCES are similarly except a little strength at 2929 cm^{-1} for CHCES. This may attribute to the introduction of methane groups. It also can be seen that CHCES has a broad vibration of δH_2O at 1656 cm^{-1} while CAES shows the coupling of δN–H and δH_2O at 1648 cm^{-1}. The XRD diagrams of raw and chemically modified starch are shown in Fig. 3. The XRD pattern of native starch and ES have the same characteristic peaks at 2θ of 15°, 18°and 23°. Compared with native starch, the intensity of ES is much lower due to the effect of enzymolysis. By introduction of more epoxy groups, the intensity of CHCES is decreased compared with CES. Peaks of CAES have a slightly increase as the introduction of diethylenetriamine groups.

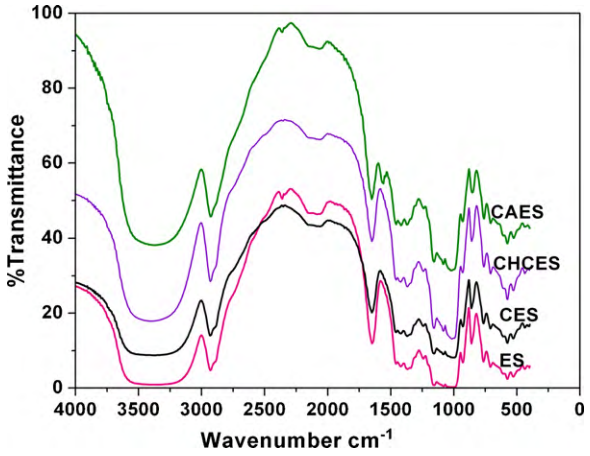

Fig. 2. FTIR spectra of ES and its derivatives.

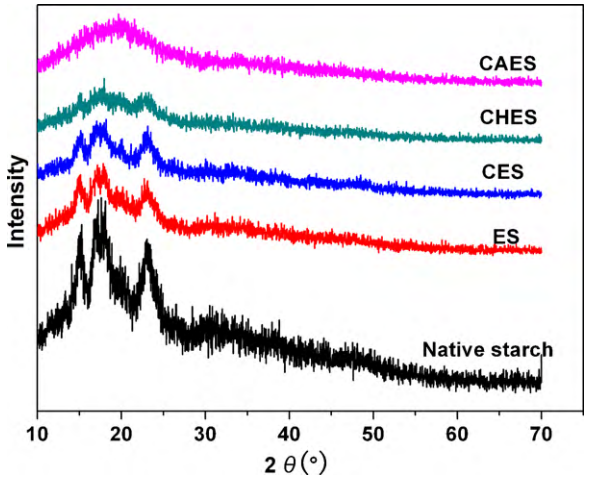

Fig. 3. X-ray diffraction patterns of native starch and its derivatives.

3.2. Sorption kinetics

Dependencies of the q_t values versus the contact time for the sorption of four acid dyes on CAES are shown in Fig. 4(a). The adsorption processes were rapid in the initial stage and level off over a short time scale. Similar trends were obtained shown in Fig. 4(b) for dyes onto CAS. In order to further analyze the kinetic mechanism that controls the adsorption process, the Lagergren

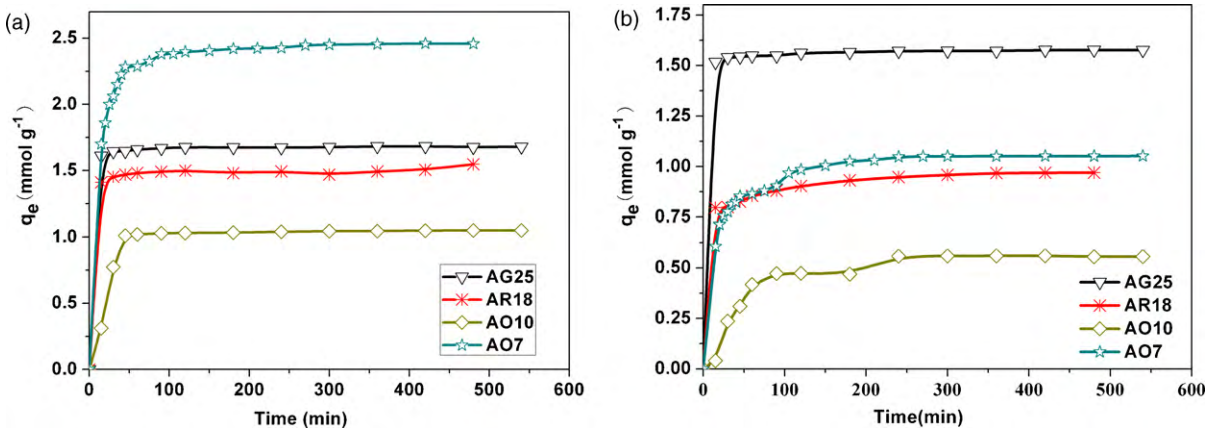

Fig. 4. Effect of adsorption time on dye adsorption by CAES (a) and CAS (b).

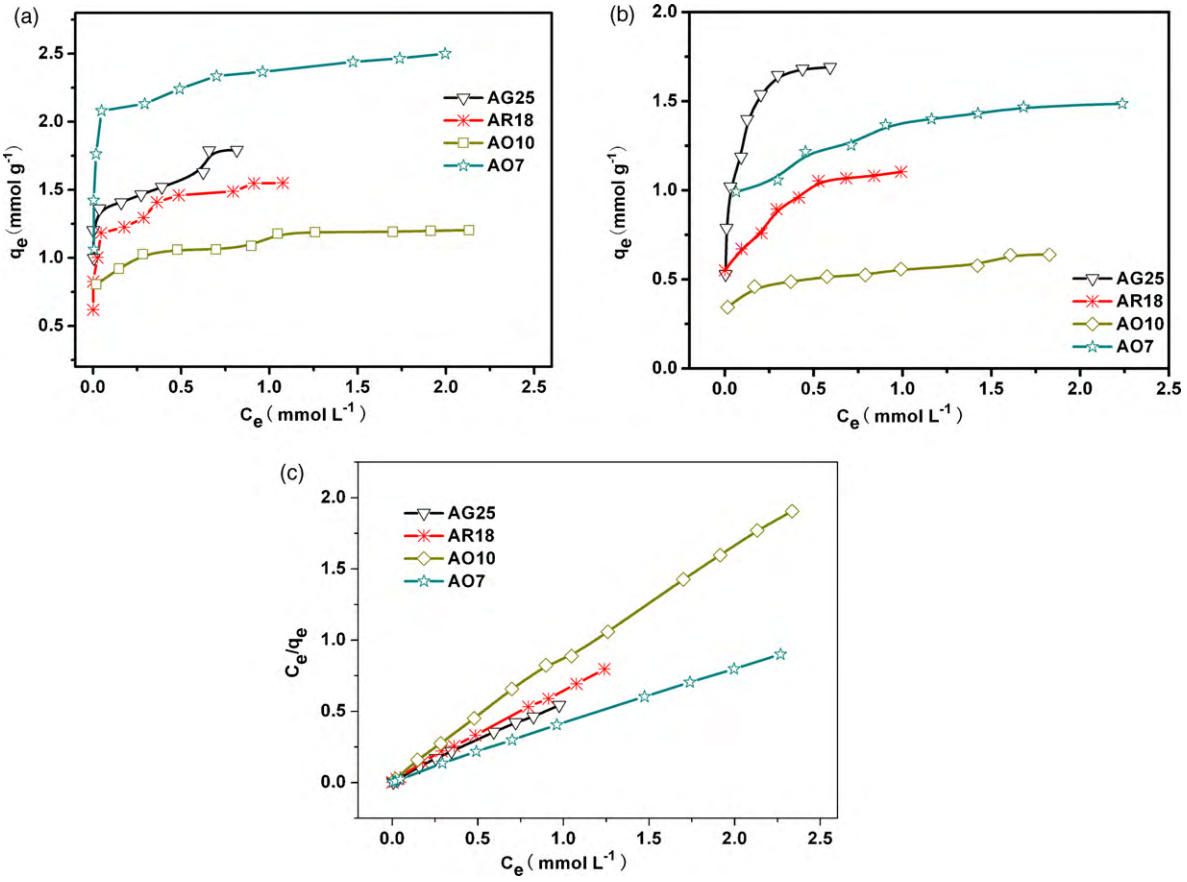

Fig. 5. Effect of initial concentration on acid dyes adsorption by CAES (a) and CAS (b) and Langmuir isotherm linear plots for the sorption of acid dyes onto CAES (c).

pseudo-first order model [30] and the pseudo-second-order model [31] are employed to interpret the experimental data shown as Eqs. (2) and (3).

$$\text{pseudo-first-order}: \quad \frac{1}{q_t} = \frac{k_1}{q_e t} + \frac{1}{q_e} \tag{2}$$

where k_1 (min^{-1}) is the pseudo-first-order adsorption rate constant, q_t is the amount adsorbed at time t (min), and q_e denotes the amount adsorbed at equilibrium, both in mmol g^{-1}.

$$\text{pseudo-second-order}: \frac{t}{q_t} = \frac{1}{k_2 q_e^2} + \frac{1}{q_e} t \tag{3}$$

The initial adsorption rate h (mmol g^{-1} min^{-1}) can be determined from k_2 and q_e values using

$$h = k_2 q_e^2 \tag{4}$$

where q_t and q_e are the amount adsorbed at time t and at equilibrium (mol g^{-1}), respectively; k_2 is the pseudo-second order rate constant for the adsorption process (g mg^{-1} min^{-1}).

Parameters obtained by linear regression are reported in Table 2. As can be seen that pseudo-first-order model did not fit the data well as the low values of R^2. Then, kinetics of the four acid dyes on CAS/CAES was analyzed using pseudo-second-order (Ho and McKay model). Results show that adsorption systems followed the

Table 2
Kinetic parameters for acid dyes adsorption by CAES and CAS.

Pseudo-first-order model						
Dyes	CAES			CAS		
	k_1 (min^{-1})	q_1 (mmol g^{-1})	R^2	k_1 (min^{-1})	q_1 (mmol g^{-1})	R^2
AG25	0.684	1.681	0.962	0.615	1.573	0.868
AR18	1.019	1.506	0.705	7.371	0.975	0.949
AO10	42.74	1.382	0.811	47.75	0.647	0.943
AO7	7.018	2.545	0.980	11.07	1.068	0.973

Pseudo-second-order model								
Dyes	CAES				CAS			
	k_2 (min^{-1})	h (mmol g^{-1} min^{-1})	q_2 (mmol g^{-1})	R^2	k_2 (min^{-1})	h (mmol g^{-1} min^{-1})	q_2 (mmol g^{-1})	R^2
AG25	6.259	17.71	1.682	1.000	3.332	8.318	1.580	1.000
AR18	1.244	2.882	1.522	0.999	0.113	0.110	0.986	1.000
AO10	0.105	0.124	1.085	0.997	0.0065	0.002	0.602	0.996
AO7	2.523	15.60	2.518	0.999	0.098	0.001	1.095	0.999

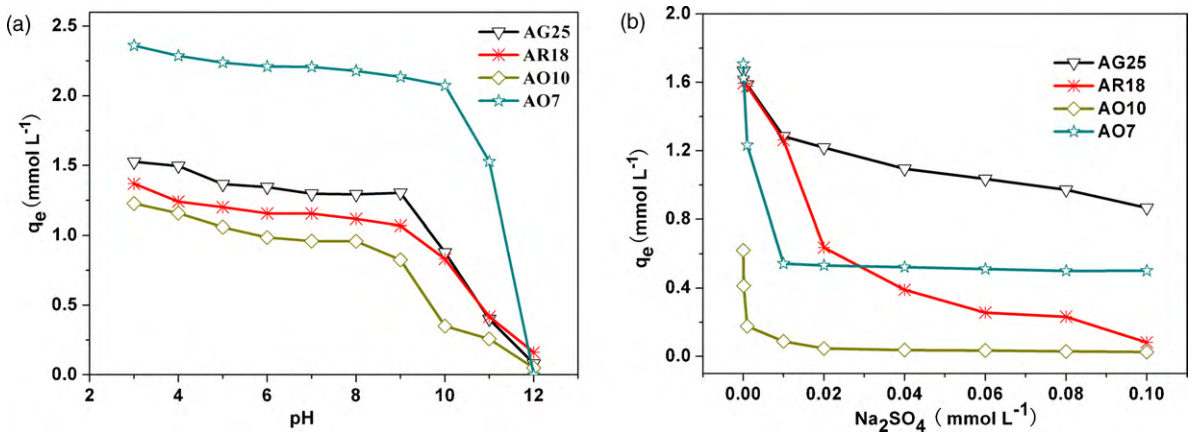

Fig. 6. Effect of electrostatic interaction on the adsorption of four acid dyes onto CAES: (a) for the effect of pH and (b) for the effect of solution ionic strength.

Ho and McKay equations for the entire adsorption period, with R^2 higher than 0.996. The calculated q_e values from this model are also in good agreement with the experimental data. Kinetics of dyes sorption on CAS/CAES followed the pseudo-second-order model, suggesting that the rate-limiting step may be chemisorption [31,32]. The results also show that values for h are much higher onto CAES than that onto CAS. As CAES is characterized by its high percentage of amine groups, the higher h values of CAES confirms that the adsorption of dye takes place probably via surface exchange reactions until the surface functional sites are fully occupied; thereafter dye molecules diffuse into the polymer network for further interactions (such as hydrogen bonding, hydrophobic interactions). Further analysis of the initial sorption rate shows that the sequence of h is: AG25 > AR18 > AO7 > AO10 for the dyes on CAS. However, the sequence of h for CAES is AO7 > AG25 > AR18 > AO10. This result indicates that chemical structure of AO7 presents more compatible size, steric arrangement with CAES comparing other acid dyes. As all the experiments were made in the same conditions except for the adsorbent with different surface morphology and grafting ratio, it can be verified that the molecular size and stereostructure formed by acid dyes and adsorbents are other main factors affecting the sorption rate.

3.3. Sorption isotherms

Adsorption isotherms can describe how adsorbates interact with adsorbents and so are critical in optimizing the use of adsorbents. In this study, experimental data of four acid dyes adsorbed on CAES and CAS equilibrium isotherms are shown in Fig. 5(a) and (b), respectively. It can be clearly seen that all the sorption capacities strongly increase with the initial concentration and level out at higher adsorbate concentrations due to the saturation of the sorption sites on the adsorbents. With the aim to know the behaviors of the sorption, two isotherms (Langmuir and Freundlich isotherms) are employed to fit the experimental data.

Langmuir adsorption isotherm was first proposed to describe the adsorption of gas molecules onto metal surfaces in one molecule thickness [33]. It has also been successfully applied in many real monolayer sorption processes. In this study, sorption data was analyzed according to the linear form (Eq. (5)) of Langmuir isotherm. The linear plots of specific sorption C_e/q_e against the equilibrium concentration C_e for the four dyes onto CAES are shown in Fig. 5(c) and relation coefficients are shown in Table 3.

$$\frac{C_e}{q_e} = \frac{1}{K_L q_m} + \frac{1}{q_m} \tag{5}$$

where q_e and C_e are the amount adsorbed (mmol g^{-1}) and the adsorbate concentration in solution (mmol L^{-1}), both at equilibrium. K_L (L g^{-1}) is the Langmuir constant and q_m (mmol g^{-1}) is the maximum adsorption capacity for monolayer formation on adsorbent. The experimental data were also analyzed using the linear form (Eq. (6)) of the Freundlich isotherm, which is applicable to heterogeneous surface adsorption with a uniform energy distribution [34]. The relation constants are presented in Table 3.

$$\ln q_e = \ln K_F + \frac{1}{n} + \ln C_e \tag{6}$$

Table 3
Sorption isotherm constants for acid dyes onto CAES and CAS.

Langmuir sorption isotherms constants						
Dyes	CAES			CAS		
	K_L (L mmol^{-1})	q_m (mmol g^{-1})	R^2	K_L (L mmol^{-1})	q_m (mmol g^{-1})	R^2
AG25	38.63	1.798	0.997	43.86	1.751	0.997
AR18	39.57	1.570	0.998	15.98	1.159	0.991
AO10	15.01	1.242	0.998	9.452	0.650	0.987
AO7	27.55	2.521	0.999	6.409	1.577	0.990
Freundlich sorption isotherm constants						
Dyes	CAES			CAS		
	K_F (mmol$^{1-1/n}$ L$^{1/n}$ g^{-1})	$1/n$	R^2	K_F (mmol$^{1-1/n}$ L$^{1/n}$ g^{-1})	$1/n$	R^2
AG25	1.759	0.567	0.933	0.903	0.291	0.877
AR18	1.120	0.434	0.934	0.398	0.157	0.976
AO10	1.094	0.124	0.967	0.266	0.124	0.958
AO7	1.108	0.872	0.833	1.315	0.130	0.803

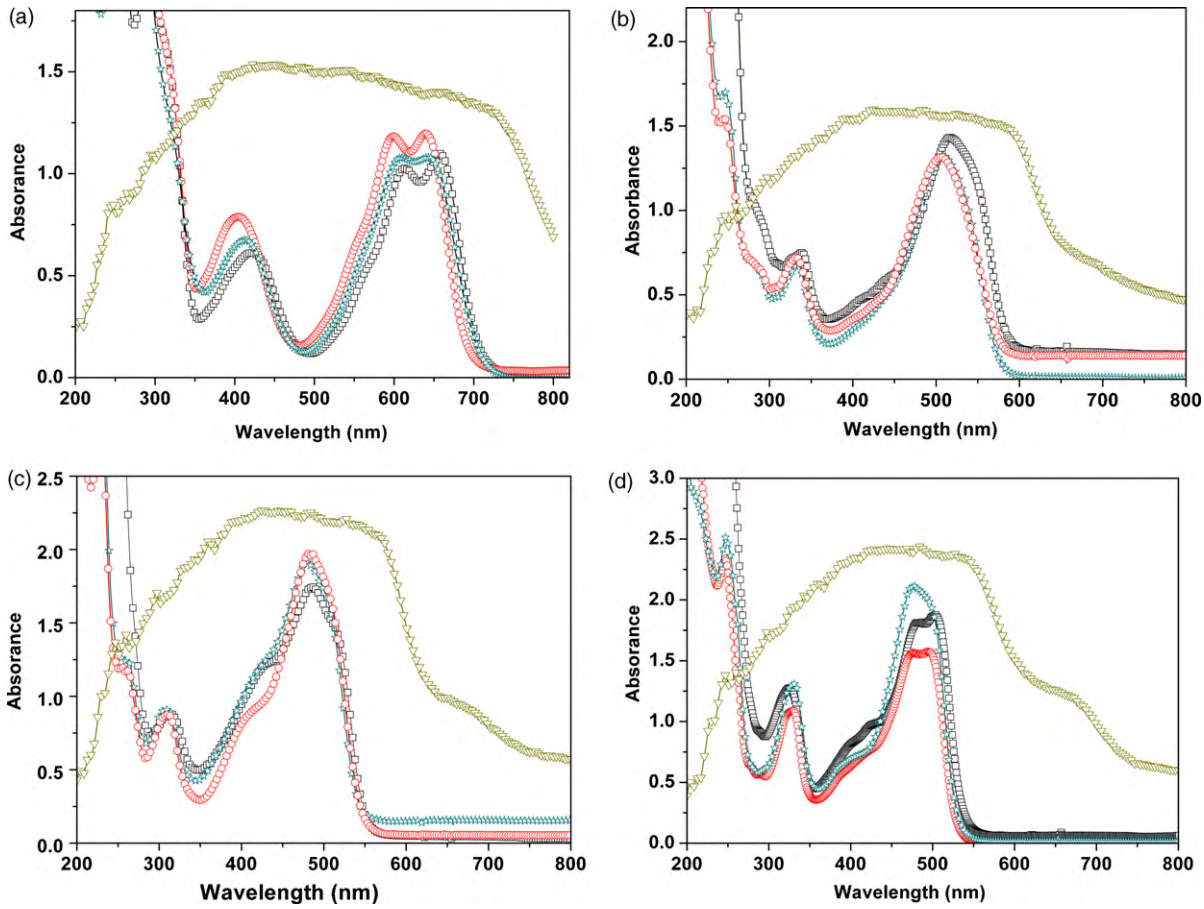

Fig. 7. Electronic absorption spectra of 10–5 mol L^{-1} solutions (by transmittance) of acid dyes ((a) for AG25, (b) for AR18, (c) for AO7 and (d) for AO10, respectively.) in deionized water (○), MeOH (☆), and DMSO (□) and adsorbed on CAES (▽) by diffuse reflectance.

where q_e is the amount adsorbed at equilibrium (mmol g^{-1}), C_e is the liquid-phase sorbate concentration at equilibrium (mmol L^{-1}), K_F is the Freundlich constant (mmol$^{1-1/n}$ $L^{1/n}$ g^{-1}), and $1/n$ is the heterogeneity factor.

Fig. 5(c) shows the Langmuir equilibrium isotherms for the adsorption of acid dyes onto CAES. The plots of C_e/q_e versus C_e in the insets give straight lines, revealing that sorption processes of the four acid dyes onto CAES obey the Langmuir isotherm. Sorption courses onto CAS also take this trend. As illustrated in Table 3, the correlation coefficients R^2 for the Freundlich isotherms are relatively lower. Sorption capacities calculated from Langmuir isotherm follow the sequence: AG25 > AO7 > AR18 > AO10 onto CAS, but AO7 > AG25 > AR18 > AO10 onto CAES. In addition, the monolayer sorption capacities for the acid dyes on CAES are all higher than that onto CAS, especially for AO10 and AO7. The amount of the increasing is 0.047, 0.411, 0.592, 0.944 mmol g^{-1} for AG25, AR18, AO10 and AO7, respectively. This trend is consistent with the molecular size since smaller molecular size not only increases the

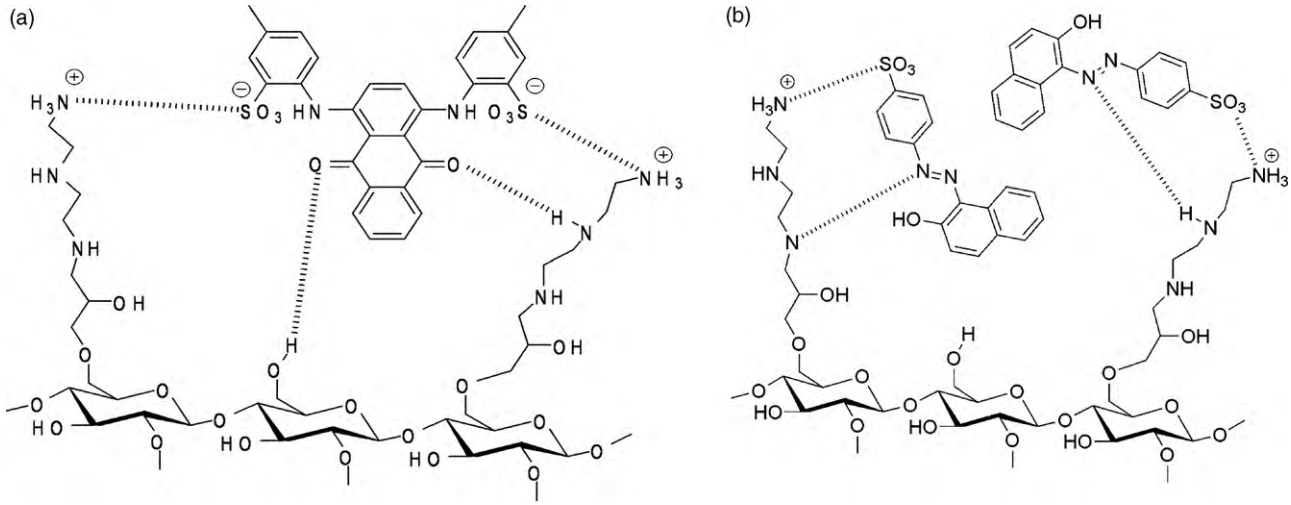

Fig. 8. Interaction models of AG25 (a) and AO7 (b) onto CAES.

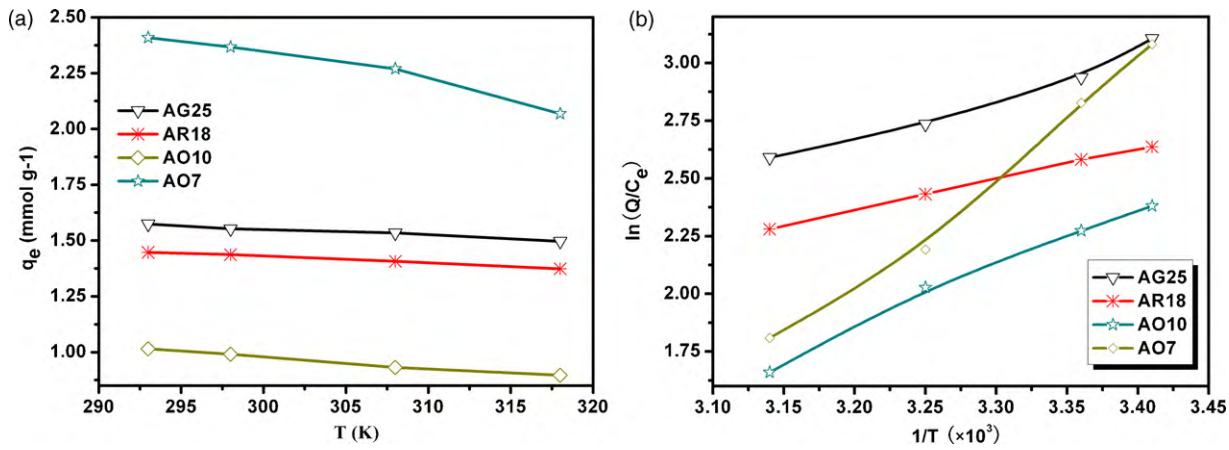

Fig. 9. Effect of adsorption temperature on dye adsorption by CAES (a) and $\log(Q/C_e) - 1/T$ for acid dyes onto CAES (b).

concentration of dye on the surface of the CAES particle but also enables a deeper penetration of dye molecules into the internal pore structure of CAES. Besides, steric effect is another important factor influencing the sorption capacity. The $-NH_3$group of CAS/CAES is the active site to uptake acid dyes. However, the increase in the grafting ratio does increase the steric hindrance for the larger dye molecule to diffuse through the adsorbents. Similar results were reported by Yilmaz et al. and Chiou and Li for adsorption of dyes on CDP polymers and chitosan, respectively [35,36].

3.4. Adsorption mechanism of acid dyes onto CAES

3.4.1. Electrostatic interaction

As all the dyes used in this study have sulfonic acid groups (Fig. 1), which enhanced their solubility in water, electrostatic interactions may be an important factor to be relevant [37]. To investigate the contribution of electrostatic interactions, we initially studied the effect of initial pH in the range of 3–12. Fig. 6(a) depicts the effect of pH on the adsorption. It shows that the sorption capacities diminish slowly from pH 3 to pH 9 and decrease sharply in the basic solutions from pH 10 to pH 12. This result demonstrates that the sorption could occur between sulfonic acid groups (SO_3^-) and protonated amine ($-NH_3^+$) groups. The large reduction in dye adsorption at highly basic conditions can be attributed to the electrostatic repulsion between the deprotonated $-NH_2$ of CAES and negatively charged dye molecules. Moreover, at lower pHs, more amine groups are protonated, with a high charge density along the starch chains, it adopts an extended conformation as the electrostatic repulsion effect that are good for sorption. On the contrary, the dyes cannot deposit well.

To further verify the importance of electrostatic interactions on the sorption process, effect of ionic strength was also investigated. As shown in Fig. 6(b), sorption capacities of acid dyes on CAES decrease upon addition of small quantities of sodium sulfate via screening the coulombic potential between the dyes and charged adsorbents, indicating chemisorption mechanisms of the sorption courses [38]. However, the decrements are different among the dyes. Sorption capacities descend steeply to small values for AR18 (0.0817 mmol L^{-1}) and AO10 (0.0259 mmol L^{-1}) but present little change for AG25 (0.867 mmol L^{-1}) and AO7 (0.501 mmol L^{-1}) as the concentration of sodium sulfate increased from 0.01 to 0.1 mol L^{-1}. This can deduce that attachment of sulfonic acid groups on the benzene rings (AG25, AO7) with $-NH_3^+$ of the CAES appeared to be stronger than those on the naphthalene rings (AO10, AR18) for the high intensity of negative charge distribution. This is an interesting finding, since many authors have found similar trend that anionic dyes with sulfonic acid groups on benzene rings are easily to be adsorbed than those on naphthalene rings [39,40], but have no explanation for it. It also can be seen that AG25 which contains two sulfonic acid groups on the benzene rings suffers less sorption capacity reduction (0.801 mmol L^{-1}) comparing with AO7 (1.206 mmol L^{-1}) with only one sulfonic acid group on its molecule, indicates that electrostatic interaction is of importance to the sorption.

3.4.2. Hydrogen bonding and steric hindrance

In order to evaluate the contribution of hydrogen bonding between acid dyes and adsorbent, several types of solvents (water, methanol, and dimethylsulfoxide) were employed. The results are shown in Fig. 7. The sorption spectrum of AG25

Table 4
Thermodynamic parameters at various temperatures for acid dyes adsorbed onto CAES.

T (K)	AG25			AR18		
	ΔG° (kJ mol^{-1})	ΔH° (kJ mol^{-1})	ΔS° (J mol^{-1} K^{-1})	ΔG° (kJ mol^{-1})	ΔH° (kJ mol^{-1})	ΔS° (J mol^{-1} K^{-1})
293	−7.485	−15.66	−27.90	−6.451	−11.182	−16.147
298	−7.346			−6.370		
308	−7.067			−6.209		
318	−6.788			−6.048		
T (K)	AO10			AO7		
	ΔG° (kJ mol^{-1})	ΔH° (kJ mol^{-1})	ΔS° (J mol^{-1} K^{-1})	ΔG° (kJ mol^{-1})	ΔH° (kJ mol^{-1})	ΔS° (J mol^{-1} K^{-1})
293	−1.291	−6.961	−19.35	−5.882	−22.15	−55.52
298	−1.195			−5.605		
308	−1.001			−5.045		
318	−0.808			−4.495		

obtained in DMSO, a non-hydrogen-bonding solvent is red shifted (λ_{max} = 658 nm) in comparison with methanol (λ_{max} = 644 nm) and water (λ_{max} = 640 nm), stronger hydrogen-bonding medium. Spectrum of AG25 absorbed on CAES is very different: the band is largely broadened toward the short wavelength and no obvious peak position can be seen. For the pH and ion strength are insensitive to the λ_{max} of dyes, this shift indicates strong hydrogen bonding between dyes and adsorbent [41]. The trend is also apparent for AR18 (λ_{max} = 517 nm in DMSO, λ_{max} = 508 nm in methanol, λ_{max} = 506 nm in water and a broad band for the AR18 adsorbed onto CAES), implied strong hydrogen bonding between AR18 and CAES. The shift of the spectra for AO10 is minished (λ_{max} = 483 nm in DMSO, λ_{max} = 476 nm in methanol, λ_{max} = 476 nm in water). And spectra of AO7 have no remarkable shift in methanol (λ_{max} = 486 nm) and a small shift in water (λ_{max} = 481 nm) comparing with the spectrum obtained in DMSO (λ_{max} = 485 nm), and band for AO7 adsorbed on CAES is much narrower comparing with the variation of AG25 onto CAES. So we can conclude that the tendency to form hydrogen bonds with CAES is AG25 > AR18 > AO10 > AO7. The forming of hydrogen bonds on one hand promoted the sorption, as the strong combination of hydrophilic functional groups between dyes and CAES; on the other hand, the present of hydrogen bonds will retard the sorption by steric hindrance. Simulating interactions with CAES are shown in Fig. 8(a) for AG25 and in Fig. 8 (b) for AO7. It can be seen that hydrogen bonds between AG25 and CAES are formed by –OH–O= and –OH–N–, taking up large space which restrict other molecules to access into the nearby active sites. By contrast, AO7 has the least hydrophilic functional groups. Moreover, the conjugated π-orbitals elongated its molecules. Therefore, –N=N– of AO7 is relatively far from the–OH of CAES, and more space is left for other molecules to reach the active sites. This can explain the result that when the grafting groups is raised, a large amount of capacity for AO7 whereas small increment for AG25.

3.5. Effect of adsorption temperature

Adsorption behaviors of dyes onto CAS and CAES at different temperatures (varied from 293 to 318 K) were also investigated, and results are shown in Fig. 9(a). It can be seen from this figure that all the adsorption capacities onto CAES are higher at relatively low temperature, indicate that this adsorption process would be exothermic. To verify the result, curves of $\log(Q/C_e)$ versus $1/T$ for the adsorption are depicted in Fig. 9(b). As the relation between $\log(Q/C_e)$ and $1/T$ is linear ($R^2 > 0.99$), the changes of apparent enthalpy (ΔH°), entropy (ΔS°) are calculated using the Van't Hoff equation:

$$\log\left(\frac{Q}{C_e}\right) = -\frac{\Delta H^\circ}{2.303RT} + \frac{\Delta S^\circ}{2.303R} \quad (7)$$

$$\Delta G^\circ = \Delta H^\circ - T\Delta S^\circ \quad (8)$$

Values of ΔH°, ΔS°, and ΔG° are listed in Table 4. Negative values of ΔH° indicate that these adsorption processes are exothermic. In addition, negative values of ΔS° and ΔG° demonstrate spontaneous adsorption processes.

4. Conclusion

Native starch and enzymatic hydrolysis starch modified by diethylenetriamine with different grafting amounts can be as evidence influence on the adsorption capacities for the acid dyes (AG25, AR18, AO10 and AO7), the conclusions are as following:

1. With higher amounts of grafting groups, CAES exhibited higher adsorption capacities for all the dyes studied in this paper. Increments of the sorption capacities for the four acid dyes took the sequence of AO7 > AO10 > AR18 > AG25.
2. Adsorption processes for the four acid dyes were found to obey pseudo-second-order model and follow the Langmuir monolayer model.
3. Intermolecular interactions were revealed by studying the effects of pH, ionic strength and the contribution of hydrogen bonding. The result confirmed chemical interaction between the dyes and adsorbents. Apart from dye initial concentration, sorption time, pH and temperature discussed in this paper and most literatures, this study also showed that molecular size of the acid dyes and stereostructure formed by acid dyes and adsorbents, strength that sulfonic acid groups of the dyes combine with protonation of amino group ($-NH_3^+$) of CAES were all important factors affecting the sorption capacity. The negative value of free energy change, enthalpy change and entropy change of the adsorption confirmed that all the sorption processes were spontaneous and endothermic in nature.

Acknowledgements

This work was supported financially by the National Natural Science Foundation of China (no. 20577034). The authors thank Yang Hu (Department of Chemistry, Tongji University, Shanghai 200092, China) for assistance during this work.

References

[1] T. Robinson, G. McMullan, R. Marchant, P. Nigam, Remediation of dyes in textile effluent: a critical review on current treatment technologies with a proposed alternative, Bioresour. Technol. 77 (2001) 247–255.
[2] G. Crini, Non-conventional low-cost adsorbents for dye removal: a review, Bioresour. Technol. 97 (2006) 1061–1085.
[3] K.C. Chen, J.Y. Wu, C.C. Huang, Y.M. Liang, S.C.J. Hwang, Decolorization of azo dye using PVA-immobilized microorganisms, J. Biotechnol. 101 (2003) 241–252.
[4] G.S. Heiss, B. Gowan, E.R. Dabbs, Cloning of DNA from a Rhodococcus strain conferring the ability to decolorize sulfonated azo dyes, FEMS Microbiol. Lett. 99 (1992) 221–226.
[5] C.A. Fewson, Biodegradation of xenobiotic and other persistent compounds: the causes of recalcitrance, Trends Biotechnol. 6 (1988) 148–153.
[6] S. Seshadri, P.L. Bishop, A.M. Agha, Anaerobic/aerobic treatment of selected azo dyes in wastewater, Waste Manage. 15 (1994) 127–137.
[7] D. Pokhrel, T. Viraraghavan, Treatment of pulp and paper mill wastewater—a review, Sci. Total Environ. 333 (2004) 37–58.
[8] M. Muthukumar, D. Sargunamani, N. Selvakumar, Statistical analysis of the effect of aromatic, azo and sulphonic acid groups on decolouration of acid dye effluents using advanced oxidation processes, Dyes Pigm. 65 (2005) 151–158.
[9] A Aguedach, S. Brosillon, J. Morvan, E.K. Lhadi, Photocatalytic degradation of azo-dyes Reactive Black 5 and Reactive Yellow 145 in water over a newly deposited titanium dioxide, Appl. Catal. B 57 (2005) 55–62.
[10] I. Uzun, Kinetics of the adsorption of reactive dyes by chitosan, Dyes Pigm. 70 (2006) 76–83.
[11] R.A. Shawabkeh, M.F. Tutunji, Experimental study and modeling of basic dye sorption by diatomaceous clay, Appl. Clay Sci. 24 (2003) 111–120.
[12] Y.E. Mouzdahir, A. Elmchaouri, R. Mahboub, A. Gil, S.A. Korili, Adsorption of Methylene Blue from aqueous solutions on a Moroccan clay, J. Chem. Eng. Data 52 (2007) 1621–1625.
[13] V.K. Garg, M. Amita, R. Kumar, R. Gupta, Basic dye (methylene blue) removal from simulated wastewater by adsorption sawdust: a timber using Indian Rosewood industry waste, Dyes Pigm. 63 (2006) 243–250.
[14] A. Shukla, Y.H. Zhang, P. Dubey, J.L. Margrave, S.S. Shukla, The role of sawdust in the removal of unwanted materials from water, J. Hazard. Mater. 95 (2002) 137–152.
[15] M.Y. Chang, R.S. Juang, Adsorption of tannic acid, humic acid, and dyes from water using the composite of chitosan and activated clay, J. Colloid Interface Sci. 278 (2004) 18–25.
[16] M. Alkan, O. Demirbas, S. Celikcapa, M. Dogan, Sorption of acid red 57 from aqueous solution onto sepiolite, J. Hazard. Mater. 116 (2004) 135–145.
[17] G.M. Walker, L. Hansen, J.A. Hanna, S.J. Allen, Kinetics of a reactive dye adsorption onto dolomitic sorbents, Water Res. 37 (2003) 2081–2089.
[18] O. Ozdemir, B. Armagan, M. Turan, M.S. Celik, Comparison of the adsorption characteristics of azo-reactive dyes on mezoporous minerals, Dyes Pigm. 62 (2004) 49–60.
[19] S. Babel, T.A. Kurniawan, Low-cost adsorbents for heavy metals uptake from contaminated water: a review, J. Hazard. Mater. 97 (2003) 219–243.

[20] R.S. Blackburn, Natural polysaccharides and their interactions with dye molecules: applications in effluent treatment, Environ. Sci. Technol. 38 (2004) 4905–4909.
[21] S.M. Xu, J.L. Wang, R.L. Wu, J.D. Wang, H. Li, Adsorption behaviors of acid and basic dyes on crosslinked amphoteric starch, Chem. Eng. J. 117 (2006) 161–167.
[22] F. Gimbert, N. Morin-Crini, F. Renault, P.M. Badot, G. Crini, Adsorption isotherm models for dye removal by cationized starch-based material in a single component system: error analysis, J. Hazard. Mater. 157 (2008) 34–46.
[23] J. Benzhi, Study on the prepareation and application of cationic starch with high degree of substitution, Ph.D. dissertation, 2000, pp. 105–126.
[24] F. Delval, G. Crini, N. Morin, J. Vebrel, S. Bertini, G. Torri, The sorption of several types of dye on crosslinked polysaccharides derivatives, Dyes Pigm. 53 (2002) 79–92.
[25] R.M. Cheng, S.J. Ou, B. Xiang, Y.J. Li, Q.Q. Liao, Adsorption behavior of hexavalent chromium on synthesized ethylenediamine modified starch, J. Polym. Res. 16 (2009) 703–708.
[26] R.M. Cheng, S.J. Ou, M.J. Li, Y.J. Li, B. Xiang, Ethylenediamine modified starch as biosorbent for acid dyes, J. Hazard. Mater. 172 (2009) 1665–1670.
[27] X. Jin, M.Q. Jiang, X.Q. Shan, Z.G. Pei, Z. Chen, Adsorption of methylene blue and orange II onto unmodified and surfactant-modified zeolite, J. Colloid Interface Sci. 328 (2008) 243–247.
[28] W.H. Cheung, Y.S. Szeto, G. McKay, Enhancing the adsorption capacities of acid dyes by chitosan nano particles, Bioresour. Technol. 100 (2009) 1143–1148.
[29] Y.J. Li, B. Xiang, Y.M. Ni, Removal of Cu(II) from aqueous solutions by chelating starch derivatives, J. Appl. Polym. Sci. 92 (2004) 3881–3885.
[30] S. Lagergren, B.K. Svenska, Zur theorie der sogenannten adsorption geloester stoffe, Kungliga Svenska Vetenskapsakadmiens Handlingar 24 (1898) 1–39.
[31] Y.S. Ho, G. McKay, A comparison of chemisorption kinetic models applied to pollutant removal on various sorbents, Process. Saf. Environ. Prot. 76 (1998) 332–340.
[32] Y.S. Ho, G. McKay, Kinetic of sorption of basic dyes from aqueous solution by sphagnum moss peat, Can. J. Chem. Eng. 76 (1998) 822–827.
[33] I. Langmuir, The adsorption of gases on plane surfaces of glass, mica and platinum, J. Am. Chem. Soc. 40 (1918) 1361–1403.
[34] C.H. Giles, D. Smith, A. Huitson, A general treatment and classification of the solute adsorption isotherm. I. Theoretical, J. Colloid Interface Sci. 47 (1974) 755–765.
[35] O.E. Yilmaz, A. Sirit, M. Yilmaz, A calyx arene oligomer and two beta-cyclodextrin polymers: synthesis and sorption studies of azo dyes, J. Macromol. Sci., Pure Appl. Chem. 44 (2007) 167–173.
[36] M.S. Chiou, H.Y. Li, Equilibrium and kinetic modeling of adsorption of reactive dye on cross-linked chitosan beads, J. Hazard. Mater. 93 (2002) 233–248.
[37] G. Schüürmann, Multilinear, regression and comparative molecular field analysis (CoMFA) of azo dye-fiber affinities. 2. Inclusion of solution-phase molecular orbital descriptors, J. Chem. Inf. Comput. Sci. 43 (2003) 1502–1512.
[38] M.S. Chiou, H.Y. Li, Adsorption behavior of reactive dye in aqueous solution on chemical cross-linked chitosan beads, Chemosphere 50 (2003) 1095–1105.
[39] R.M. Cheng, S.J. Ou, B. Xiang, Y.J. Li, Q.Q. Liao, Equilibrium and molecular mechanism of anionic dyes adsorption onto copper(II) complex of dithiocarbamate-modified starch, Langmuir 26 (2010) 752–758.
[40] W.T. Tsai, C.Y. Chang, C.H. Ing, C.F. Chang, Adsorption of acid dyes from aqueous solution on activated bleaching earth, J. Colloid Interface Sci. 275 (2004) 72–78.
[41] S.B. Yamaki, D.S. Barros, C.M. Garcia, P. Socoloski, O.N. Oliveira, T.D.Z. Atvars, Spectroscopic studies of the intermolecular interactions of Congo red and tinopal CBS with modified cellulose fibers, Langmuir 21 (2005) 5414–5420.